nature food

Article

https://doi.org/10.1038/s43016-024-01004-y

Marine aquaculture can deliver 40% lower carbon footprints than freshwater aquaculture based on feed, energy and biogeochemical cycles

Received: 9 January 2023

Accepted: 17 May 2024

Published online: 21 June 2024

Check for updates

Lu Shen[1,2,13] ✉, Lidong Wu[3,4,13], Wei Wei[5,13], Yi Yang[5], Michael J. MacLeod[6], Jintai Lin[1], Guodong Song[7], Junji Yuan[8], Ping Yang[9], Lin Wu[10], Mingwei Li[11] & Minghao Zhuang[12] ✉

Freshwater aquaculture is an increasingly important source of blue foods but produces substantial methane and nitrous oxide emissions. Marine aquaculture, also known as mariculture, is a smaller sector with a large growth potential, but its climate impacts are challenging to accurately quantify. Here we assess the greenhouse gas emissions from mariculture's aquatic environment in global potentially suitable areas at 10 km resolution on the basis of marine biogeochemical cycles, greenhouse gas measurements from research cruises and satellite-observed net primary productivity. Mariculture's aquatic emissions intensities are estimated to be 1–6 g CH_4 kg^{-1} carcass weight and 0.05–0.2 g N_2O kg^{-1} carcass weight, >98% and >80% lower than freshwater systems. Using a life-cycle assessment approach, we show that mariculture's carbon footprints are ~40% lower than those of freshwater aquaculture based on feed, energy use and the aquatic environment emissions. Adoption of mariculture alongside freshwater aquaculture production could offer considerable climate benefits to meet future dietary protein and nutritional needs.

Aquaculture represents a potentially large food source to sustainably meet the protein demands of an increasingly affluent human population[1]. In 2019, the world consumed 117 million tonnes of edible aquatic products (plants excluded), with 52% from wild captures, 41% from land-based aquaculture and 7% from mariculture[2]. However, with the plateauing of wild catches[3] and high environmental impacts of land-based aquaculture[4–6], a recurring theme in recent literature is that we need to effectively expand mariculture[1,7–10], which is still at the nascent stage but has the potential to produce seafood >100 times the global demand[8,9]. Previous studies have also suggested that marine and freshwater aquaculture have similar environmental impacts because feed is the leading driver of these impacts[2]. However, these studies all neglected greenhouse gas (GHG) emissions arising from the aquatic cultivation environment, resulting in inadequate evaluation of the carbon footprints of different aquaculture types[2,11,12], which will be addressed in this study.

Present-day aquaculture still heavily relies on freshwater systems, which represent a substantial anthropogenic source of methane (CH_4) and nitrous oxide (N_2O) due to increasing nutrient loadings from intensive aquafeeds[5,13] in the aquatic environment. Only a small fraction (11–36%) of nutrients in aquafeeds consumed by fish can be converted to harvested biomass, with the remainder excreted into waters[14,15] and partly transformed to CH_4 and N_2O by microbes[6]. Previous studies showed that global freshwater aquaculture emits 6–14 Tg yr^{-1} of CH_4 and 37–150 Gg yr^{-1} of N_2O (refs. 6,15–17). On the other hand, little is known about the GHG emissions during mariculture operations owing

A full list of affiliations appears at the end of the paper. ✉e-mail: lshen@pku.edu.cn; zhuangminghao@cau.edu.cn

to the scarcity of direct measurements. So far, flux measurements of CH_4 and N_2O have been obtained in only a few land-based mariculture ponds[18]. Whether the GHG emissions intensities deduced from these small-scale land-based mariculture studies also apply at the global scale for offshore mariculture is still unknown, but such knowledge is critically important for making decisions of future aquaculture development to meet international sustainability targets.

In this Article, we aim to quantify GHG emissions intensities from offshore mariculture's aquatic environment in global potentially suitable areas, by applying the theory of marine biogeochemical cycles to GHG measurements from research cruises and satellite-observed net primary productivity (NPP). We focus on the two primary GHGs, CH_4 and N_2O, from the aquatic environment[6]. Substantial carbon dioxide (CO_2) emissions associated with mariculture would be typically related to land use changes[6,12], but these changes can be mitigated by minimizing the impacts on seafloor ecosystems through careful selection of farm sites, low-density farming and environment-friendly practices[12,19]. Lastly, we evaluate the carbon footprints (CO_2, CH_4 and N_2O) of both freshwater and marine aquaculture, considering emissions from feed, energy use and the aquatic environment. These results can help inform future developing strategies of aquaculture to meet increasing fish protein needs with reduced environmental impacts.

Results

Ocean carbon and nitrogen cycling in mariculture regions

We focus on offshore regions (near-shore and shelf areas with seafloor depths <200 m) where mariculture farms can be anchored to the seafloor at acceptable expense[20]. Finfish, crustaceans and molluscs are important groups in mariculture, with the first two requiring large amounts of aquafeeds, leading to additional GHG emissions[21,22]. Following Gentry et al.[8], we constrain suitable farming areas (Supplementary Fig. 1) for each mariculture species to regions with moderate sea surface temperature ranges, high dissolved oxygen levels and low shipping traffic. Throughout this paper, we report errors as 90% confidence intervals (CIs).

According to ocean carbon cycling (Fig. 1a), the dominant source of CH_4 in mariculture areas is the organic matter that sinks to seafloor in a low-oxygen environment[23], which is directly related to ocean NPP. Produced methane is ventilated to the atmosphere by diffusion and ebullition[24], and deeper water depths can substantially increase the fraction of dissolved and oxidized methane along these two ventilation pathways[25–27]. Applying the observations of sea–air CH_4 fluxes[26], NPP[28] and chlorophyll[29] to the ocean particle export algorithm[29–31] (Supplementary Fig. 2a), surface oceans in mariculture regions (only areas suitable for offshore farming) produce 4,200 Tg NPP-C (carbon in the form of NPP) on an annual basis, of which 1,100 Tg NPP-C (~26%) is exported to the aphotic zone and 2.9 Tg CH_4-C (0.07%) is returned to the atmosphere in the form of CH_4. These calculated fluxes can well match previous estimates using modelling approaches and observations (Supplementary Fig. 2b). Such a low CH_4 conversion rate from NPP (compared with 0.5–10% in freshwater ponds[18,32]) is largely due to the existence of sulfate, a major constituent in the ocean, which can stimulate the growth of sulfate-reducing bacteria. Sulfate-reducing bacteria can compete with methane-producing microbes for the same substrates[33,34], thereby suppressing methane production (more details in Supplementary Text 1).

NPP is also the primary substrate for the N_2O-producing pathway in mariculture waters (Fig. 1a; more details in Supplementary Text 2). According to nitrogen cycling, both nitrification and denitrification can produce N_2O, but the former is more dominating in global net fluxes to the atmosphere[35–37]. Using marine water column and surface N_2O observation, Battaglia and Joos[38] quantified that 95.5% of sea–air N_2O emissions are from nitrification. Meanwhile, nitrification is light inhibited, and it mainly occurs below the euphotic zone[23], using ammonium from the remineralization of organic matter as the substrate (produced mainly by NPP). Therefore, hotspots of N_2O emissions in potential mariculture areas are often found in coastal upwelling regions (for example, the Eastern Boundary Upwelling Systems; Supplementary Fig. 3), which can sustain high NPP by bringing nutrition-rich water into the euphotic layer[39–42]. A lower oxygen concentration can enhance the N_2O yield through nitrification[38]. However, if the oxygen level falls under 5–10 μmol l^{-1} (or in the suboxic zone), usually caused by excessive microbial degradation of organic matter, denitrification will become the primary N_2O-producing pathway[43]. However, such a low-O_3 environment harms fish's fitness[8] and has been excluded from our potential mariculture areas. Here we further demonstrate that the modelled N_2O production from the nitrification yield[38] and dissolved oxygen concentrations[44] in aphotic zones are highly correlated with N_2O fluxes measurements in the surface ocean ($R = 0.78$) (Supplementary Figs. 4 and 5). This further supports our assumption that nitrification using NPP as the substrate is the primary N_2O-producing pathway in near-shore and shelf oceans. According to biogeochemical cycles, 740 Tg of nitrogen will be assimilated in NPP in mariculture regions annually, 190 Tg (26% of NPP) is exported to aphotic zones and 0.26 Tg (~0.04% of NPP) is released to the atmosphere in the form of N_2O. In this work, we calculated mariculture's GHG emissions intensity (EI) from the aquatic environment as a function of CH_4's and N_2O's production efficiencies from NPP, aquafeed element composition and feed conversion ratios (FCR; Fig. 1b). Here, the underlying logic is to convert aquafeeds, excluding the part transformed to fish biomass, to equivalent NPP (NPP_e), and NPP_e can be further related to CH_4 and N_2O emissions. Results from a variety of aquaculture systems show that only a small fraction of carbon and nitrogen (<1/3) from feeds can be directly converted to fish biomass, with the remainder excreted to waters through metabolism (for example, respiration, ammonia excretion across gills, and faeces)[15,45] (Supplementary Fig. 6). Thus, NPP_e should include unconsumed feeds, fish's faeces and newly produced NPP (NPP_{new}) by phytoplankton using excreted ammonia[15]. Considering that the particle size of NPP_e is different from oceanic NPP, we estimate the lower and upper bound of its export efficiency out of the euphotic zone as follows. For the lower bound, we assume that all NPP_e resembles the behaviours of NPP, which means ~26% of NPP_e is exported into aphotic zones and participates in the biochemical production of CH_4 and N_2O (Supplementary Figs. 7 and 8a). For the upper bound, we assume all particulate waste (unconsumed feeds and faeces) can quickly sink to the seafloor, and all NPP_{new} can enter the aphotic zone (Supplementary Figs. 7 and 8b). These upper and lower bounds of export efficiencies will later determine the range of GHG emissions in the aquaculture system (Methods and Supplementary Figs. 7 and 8).

GHG production efficiencies in potential mariculture areas

Figure 2 shows global oceanic CH_4 production efficiencies from NPP at a resolution of 10 km in offshore mariculture areas. The production efficiencies, measured as the fraction of carbon released to the atmosphere in the form of CH_4 relative to carbons in NPP (equation (6)), are relatively low in high-latitude (>45° N/S) cold regions (0.001%). It increase sharply towards the tropics, especially along the coastlines, typically ranging from 0.01% to 0.1% and occasionally reaching 0.5% in tropical Southeast Asia (more details in Supplementary Fig. 9a). Such a dependence on temperature is likely because microbial methane production (methanogenesis) is more sensitive to temperature than microbial oxidation (methanotrophy), consistent with previous observations in land aquatic systems[46]. Overall, the production efficiencies also strongly inversely correlate with seafloor depths ($R = -0.88$), from 0.08% in the depth of 0–50 m to <0.002% in the depth of >100 m (Supplementary Fig. 9b). This strong dependence on depth reflects the important role of the seafloor as a substantial source of CH_4 to the surface ocean. This is because increased water depths can increase the fraction of methane oxidized and dissolved in the surrounding waters along the ventilation paths from seafloor to the atmosphere, through ebullition and diffusive gas transfer.

https://doi.org/10.1038/s43016-024-01004-y

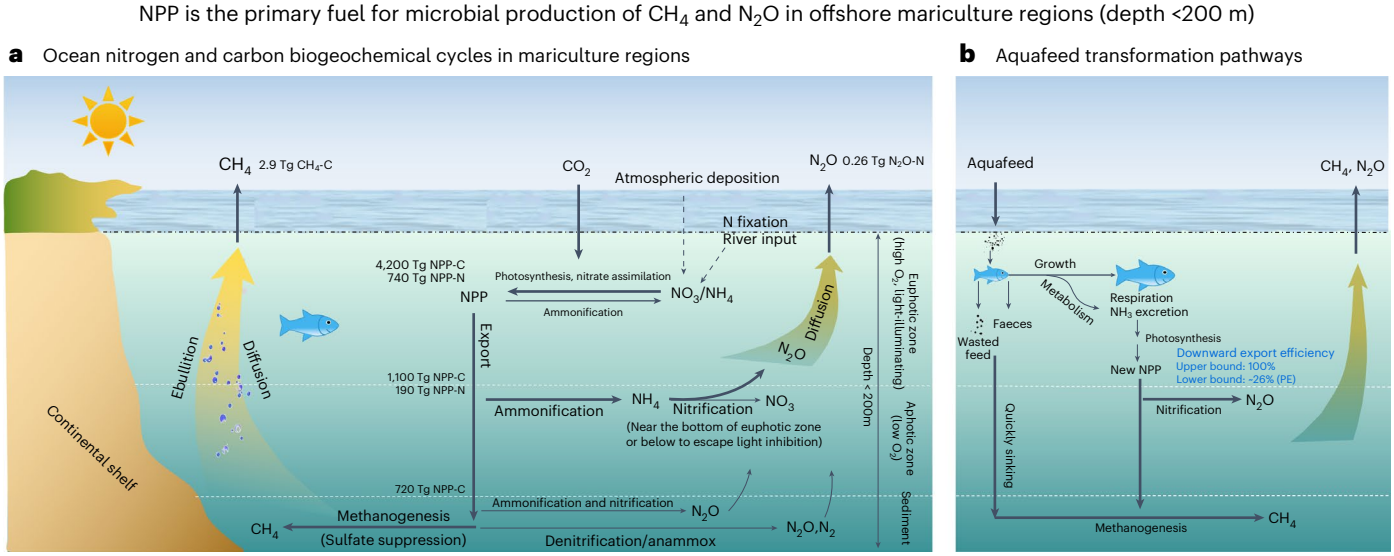

Fig. 1 | Nitrogen and carbon biogeochemical cycles in mariculture regions and aquafeed transformation in the aquaculture system. a, Formation and emission of CH_4 and N_2O in mariculture regions. The bold lines depict the primary CH_4/N_2O production and emission processes in areas suitable for offshore mariculture farming. The carbon in the form of NPP (NPP-C) is obtained from satellite observations[28], and scaling by the N:C mass ratio yields the nitrogen in the form of NPP (NPP-N). The fraction of NPP exported out of the euphotic zone is estimated by applying the observations of sea–air CH_4 fluxes[26], NPP[28] and chlorophyll[29] to the ocean particle export algorithm[29–31]. **b**, Aquafeed transformation in mariculture systems. The lower bound of export efficiency of newly produced NPP is assumed to be PE, calculated using equation (3). More details of the carbon and nitrogen utilization efficiency along different pathways can be found in Supplementary Fig. 8.

Figure 2 also shows oceanic N_2O production efficiencies, defined as the fraction of nitrogen released to the atmosphere in the form of N_2O relative to nitrogen in NPP (equation (7)). They exhibit similar features with CH_4 regarding latitudes: high efficiencies of N_2O production are present in tropical shelf regions, especially in tropical southeast Asia, with the highest values often exceeding 0.05% (Supplementary Fig. 9c). Although coastal upwelling systems are usually hotspots of sea–air N_2O fluxes[39,42], their N_2O production efficiencies (normalized by NPP) are not higher than their latitudinal counterparts (Supplementary Fig. 10). Compared with CH_4, the N_2O's production efficiencies are less dependent on water depths, ranging from 0.01% to 0.05% (Supplementary Fig. 9d). This is because most N_2O is produced by nitrification in the water column below the bottom of the euphotic zone and is biochemically stable after it ventilates into the euphotic zone[23,47,48].

GHG flux rates in different aquaculture types

We gathered reported GHG fluxes measured in 107 sites and sources, including 61 observations from freshwater systems, 37 measurements from land-based mariculture ponds, 8 campaigns in one offshore mariculture bay[49] (4 years, each campaign sampled >20 locations) and global reconstructed GHG flux (~25 km resolution) from research cruises data[26,39] (Source Data Fig. 3). Based on these results, we examined typical GHG emission features for different aquaculture systems and the potential drivers of their variability. We also compiled a worldwide database of CH_4 from freshwater aquaculture systems by multiplying these fluxes with aquaculture areas[6], which yields the global total to be 7.2 ± 1.7 Tg yr^{-1} of CH_4 and 29 ± 6 Gg yr^{-1} of N_2O for 2014 (Supplementary Table 1). The number of observations used for inventory compilation here is >2 times that in two recent studies[6,16], and the magnitude of CH_4 emissions is comparable to Yuan et al.[6] (6 Tg yr^{-1}) and lower than Rosentreter et al.[16] (14 ± 19 Tg yr^{-1}) (Supplementary Table 2).

The synthesized data show that CH_4 fluxes in the rice fish and pond (extensive and semi-intensive) systems are 12.5 (3–36) and 10.3 (0.5–25) mg CH_4 m^{-2} h^{-1} during the crop period, the highest among all aquaculture types (Fig. 3a). In mariculture, the results reveal an emergent pattern of decreasing methane fluxes with increasing salinity. The mean CH_4 fluxes are 11.8 (3–21) mg CH_4 m^{-2} h^{-1} in low-salinity waters (<5 ppt, or parts per thousand), comparable to those of freshwater systems, and decrease to 0.1 (0–0.3) mg CH_4 m^{-2} h^{-1} in land-based mariculture ponds with higher salinity (>10%), 0.03 (0–0.1) mg CH_4 m^{-2} h^{-1} in offshore mariculture farms and 0.04 mg CH_4 m^{-2} h^{-1} in near-shore and shelf oceans (depth <200 m). This extremely low methane flux in marine waters is consistent with the fact that the ocean emits only 9 ± 3 Tg CH_4 yr^{-1} (ref. 26), two orders of magnitude smaller than these land ecosystems (for example, 150 Tg CH_4 yr^{-1} in freshwater wetlands[50] and 56–151 Tg CH_4 yr^{-1} in lakes[16]). These results highlight the critical role of salinity in suppressing methane fluxes (R = −0.81; Fig. 3a), implying that offshore mariculture could considerably reduce methane emissions from the aquatic environment.

Similarly, freshwater systems also have the highest average N_2O fluxes during the crop period, with 38 (20–80) μg N_2O m^{-2} h^{-1} in rice fish systems and 34 (2–82) μg N_2O m^{-2} h^{-1} in freshwater ponds). Meanwhile, averaged N_2O fluxes are 11 (1–21) μg m^{-2} h^{-1} in land-based mariculture ponds and 4 μg m^{-2} h^{-1} in near-shore and shelf oceans, exhibiting a slightly negative dependence on salinity (P = 0.04; Fig. 3b), which is consistent with previous findings[51,52]. The much lower N_2O fluxes have been observed under a high-salinity environment (>15 ppt) due to stronger inhibitory effects on the conversion of NH_4^+ to N_2O (ref. 53), the toxicity of multiple organic carbon pounds and ions (chloride, hydrosulfide and so on)[23] and decreasing microbe's abundance and activities[54–56]. Lower salinity (<10–15 ppt) has been reported to enhance N_2O fluxes in a fraction but not all of previous studies[51–53,57], and this is not evidently observed in Fig. 3b, probably because the inter-comparison among different aquaculture systems is affected by factors such as distinct culture species, different operation practices, biochemical properties and too few observations.

GHG emissions intensity from the aquatic environment

Figure 3c displays CH_4 EI due to microbial production in the aquatic environment of three aquaculture systems. For every kilogram of edible production, CH_4 emissions are 323 ± 77 g in freshwater systems (details in Supplementary Table 3), 81 (0.1–200, depending on salinity) g in land-based mariculture ponds, and 1–6 g (lower–upper bounds) from offshore mariculture. The upper and lower bounds for

https://doi.org/10.1038/s43016-024-01004-y

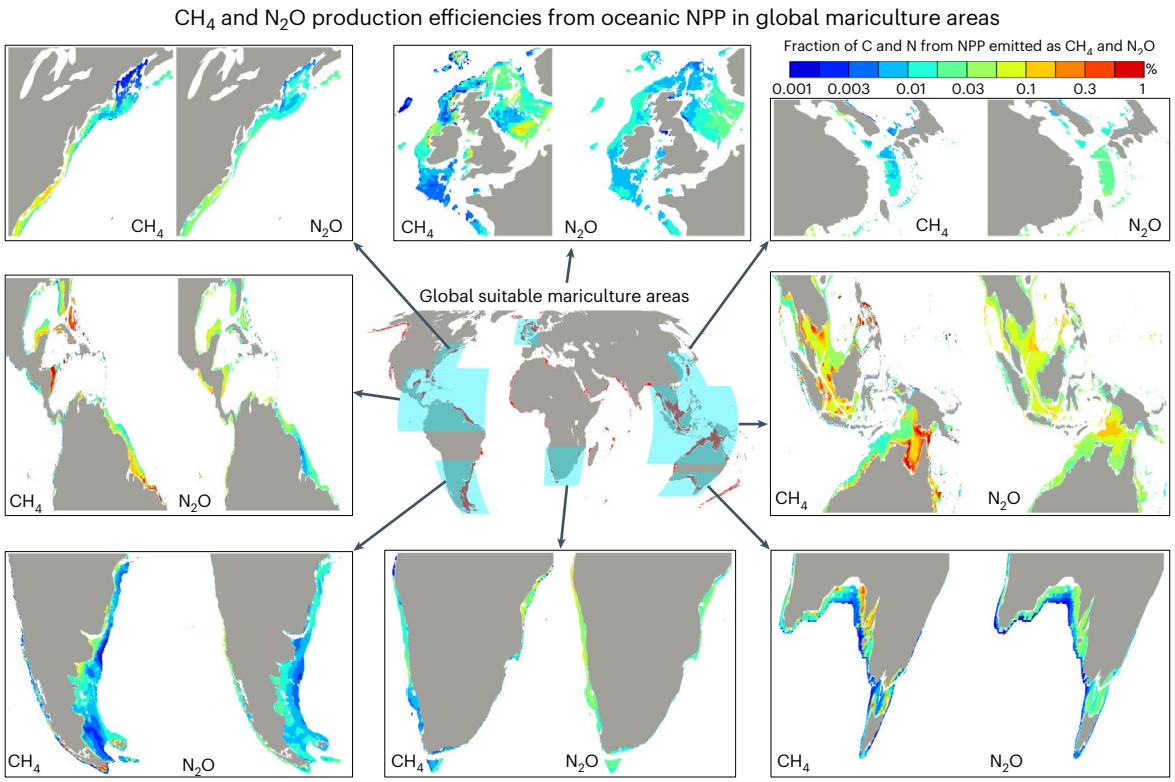

Fig. 2 | CH_4 and N_2O production efficiencies in global offshore mariculture areas. The centre map depicts locations (red areas) suitable for finfish farming (more details in Supplementary Fig. 1). Zoomed-in panels display the spatial distributions of CH_4 and N_2O production efficiencies, defined as the fraction of carbon and nitrogen emitted into the atmosphere in the form of CH_4 and N_2O from NPP (equations (6) and (7)), in eight high-potential mariculture areas in the tropics and northern/southern mid-latitudes. The complete maps of global CH_4 and N_2O production efficiencies can be found in Supplementary Fig. 9. The maps used in this figure are from an open-source software NCAR Command Language (NCL, https://www.ncl.ucar.edu/index.shtml).

offshore mariculture are calculated using different assumptions on NPP_e's export efficiency from euphotic to aphotic zones (Fig. 1b and Supplementary Figs. 7 and 8). Of the two inland aquaculture systems, the EI from land-based mariculture ponds is 75% lower than that from freshwater aquaculture, largely due to that high-concentration sulfates in marine waters can compete for electrons with these methanogens receptors, thus suppressing the gross CH_4 formation[58,59]. Offshore mariculture, usually using floating net pens anchored to seafloor in much deeper water depths, appears to have the potential to suppress CH_4 emissions by ~98% for the following reasons. First, ocean waters can sustain sulfate concentrations at a high level with little impact from rainfalls and freshwater inputs. Second, a large fraction (potentially >50%) of methane from seafloor will be oxidized and dissolved along its ventilation path to the atmosphere[25–27]; thus, the emissions intensities inversely correlate with seafloor depths.

Figure 3d further shows the N_2O EIs in different aquaculture systems, also displaying inhibition phenomena from high salinity. For every kilogram of edible production, N_2O emissions are 1.3 ± 0.3 g in freshwater systems, 0.2 (0–0.4) g in land-based mariculture ponds, and 0.05–0.2 g (lower–upper bounds) in offshore mariculture. The very high EI in freshwater systems partly arises from the intensive application of nitrogen fertilizer (especially in rice fish systems[6]), which can be efficiently converted to N_2O. High salinity has been reported to decrease the overall abundance of nitrifying microbes and their activities[54–56], and the marine water salinity (34 ppt) is much higher than the optimal salinity range (<15 ppt) for nitrification reported by previous studies[60–62].

Carbon footprint of aquaculture

Here we assess the life-cycle GHG (CO_2, CH_4 and N_2O) emissions of global aquaculture from the following activities: feed production (crop production, production of energy and fertilizer, and the production of non-crop feeds), energy use and aquatic environmental emissions. For non-aquatic emissions, we build on the previous work of MacLeod et al.[11] and Gephart et al.[63], and expand literature search for underrepresented species groups. For aquatic emissions, we rely on the newly updated global inventory of freshwater systems in this work (Supplementary Table 1) and use the upper bound of emissions intensity (Fig. 3c,d) for mariculture. Importantly, this life-cycle assessment (LCA) encompasses 23 species groups and separates them into freshwater and marine water ones, thereby enabling comparison of the carbon footprints of these two aquaculture types (Supplementary Tables 4 and 5).

Our result (Fig. 4) reveals that the aquatic environment, which was not adequately considered in previous LCAs[11,63], is responsible for 50–60% of GHG emissions for freshwater aquaculture species across their life cycle. Converting CH_4 and N_2O emissions to their 100-year warming potentials, aquatic emissions amount to 9.4 ± 2.2 kg CO_2e kg^{-1} CW (where 'CW' is 'carcass weight', or edible flesh), and CH_4 is the dominating contributor (96%). For freshwater finfishes, their carbon footprints lie between 14 and 19 kg CO_2e kg^{-1} CW, and the mean value, weighted by global production, is 15.2 ± 3.1 kg CO_2e kg^{-1} CW. Shrimps and prawns have higher carbon footprint (20.4 ± 4.0 kg CO_2e kg^{-1} CW) due to the greater amount of energy used in activities like pumping and aeration[11]. Consistent with previous work, farmed bivalves and plants generate the lowest GHG stresses because they have no feed-related emissions.

In comparison, with minimal GHG emitted by the aquatic environment, offshore mariculture's carbon footprint is estimated to be 9.0 ± 1.6 kg CO_2e kg^{-1} CW for finfish and 10.5 ± 1.8 kg CO_2e kg^{-1} CW for shrimps, 41 ± 10% and 48 ± 7% lower than their freshwater's counterparts, respectively (Fig. 4). Mariculture's carbon footprint primarily arises from feeds, which on average induce ~30% higher GHGs than freshwater species. This is because most mariculture finfishes are

https://doi.org/10.1038/s43016-024-01004-y

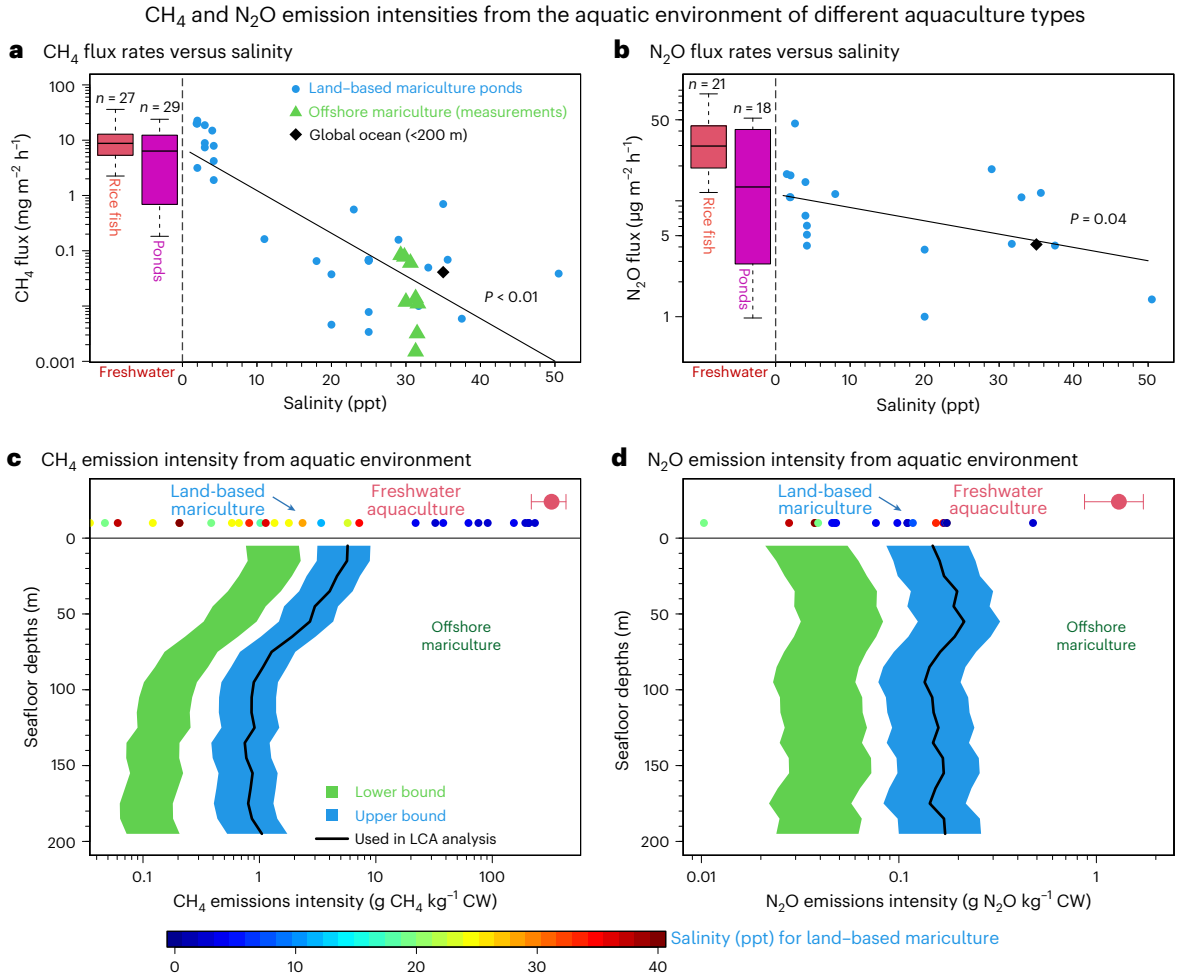

Fig. 3 | CH_4/N_2O fluxes and emissions intensities (EI) arising from the aquatic environment in different aquaculture types. a,**b**, Relationships of CH_4 (**a**) and N_2O (**b**) fluxes collected from 107 sites with salinity from two freshwater systems (rice fish and ponds), land-based and offshore mariculture, and global near-shore and shelf oceans (Source Data Fig. 3). The hinges in boxplots refer to the first and third quartiles, with the middle horizontal bar denoting the median. The whiskers indicate the range (minimum and maximum). The black lines denote the linearly fitted relationship of emission flux in the logarithm with salinity (*P* values from using two-sided *t*-tests are shown inset). **c**,**d**, Emissions intensities of CH_4 (**c**) and N_2O (**d**) from every kilogram of edible fish, binned by seafloor depths (shared area denotes 90% CI, and the bold black lines denote the mean values). Results are compared with those from the freshwater systems (error bar denotes 90% CI)[6] and land-based mariculture ponds (small circles with colours represent the salinity, and the sample size is 29 and 19 for CH_4 and N_2O, respectively). Please note that the *x* axis of **c** and **d** are in the logarithm scale. The lower bounds and upper bounds of EI are defined in the main text and Supplementary Fig. 8.

carnivorous, and they need higher protein (quality protein, for example, fishmeal) in feed formulation. Meanwhile, mariculture also needs approximately three times higher energy arising from transport and processing. Unlike freshwater aquaculture, the carbon footprint of mariculture varies considerably across different species. Finfishes with low carbon footprints (<10 kg CO_2e kg^{-1} CW) usually have lower FCR, higher edible portion and lower protein rations in feed (Supplementary Tables 4 and 5). Besides culture species selection, reducing mariculture's carbon footprints can also be achieved through innovating aquaculture technology[64]. For example, the FCR of salmon has been reduced from 2.3 in the 1970s to 1.1 in present days[63,65]. These results suggest that mariculture expansion has the potential to substantially reduce the climate impacts of present-day aquaculture.

Discussion

Here, our work quantifies GHG emissions intensities of global mariculture, based on datasets of GHG fluxes in the surface ocean and satellite-observed NPP. This approach builds on the fact that organic matter from oceanic NPP is the primary fuel for microbial production of CH_4 and N_2O in mariculture areas. We estimated GHG emissions intensities of mariculture due to emissions from the aquatic environment to be 1–6 g CH_4 kg^{-1} CW and 0.05–0.2 g N_2O kg^{-1} CW, which are >98% and >85% lower than those from freshwater systems, respectively. This is because the marine environment can suppress CH_4 formation biochemically due to high sulfate concentrations and decrease the abundance and activities of microbes due to high salinity. Increasing water depths also reduces the efficiency of GHG ventilation from seafloors to the atmosphere.

Our study does not account for potential carbon loss from the degradation of seafloor habitats after developing mariculture. In offshore mariculture, we can exclude areas of seagrass and sensitive carbon habitats wherever possible[12]. Other strategies, including climate-friendly farm designs, species selections and low-density operational practices[8], can further prevent potential damage to marine ecosystems and avoid carbon loss. We also do not evaluate the environmental impacts arising from land-derived pollution, such as atmospheric nitrogen deposition[66] and river discharge, which is likely to become important when intensive anthropogenic activities are present in coastal areas associated with mariculture development. Although low dissolved oxygen is a naturally occurring phenomenon in ocean environments (for example, in coastal upwelling systems), it can be exacerbated by intensive-feeding aquaculture and eutrophication[67].

https://doi.org/10.1038/s43016-024-01004-y

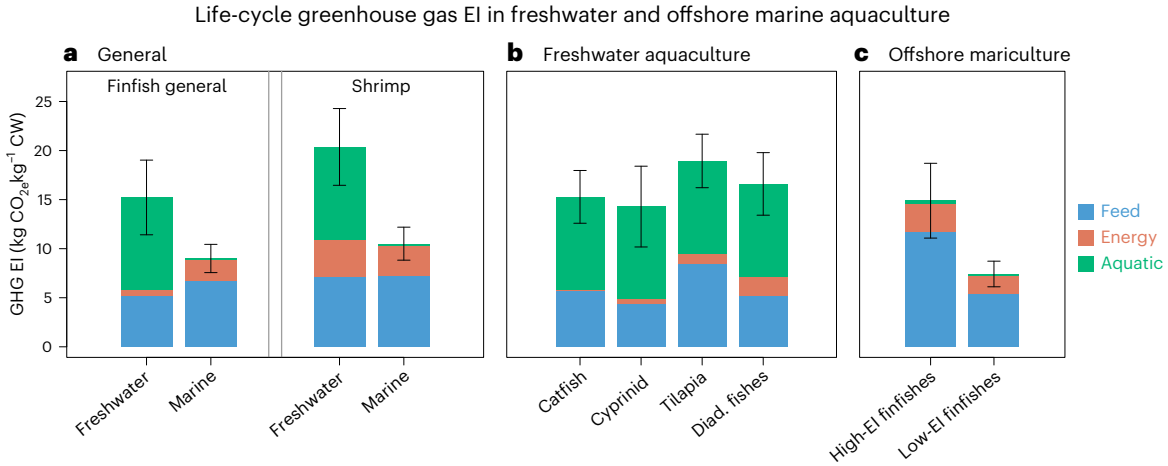

Fig. 4 | Life-cycle GHG emissions intensity in freshwater and marine aquaculture. a, GHG EI from finfish general and shrimp in the two aquaculture systems. Different colours represent GHG contributions emitted by feed, energy and the aquatic environment. **b**, GHG EI for typical finfish species in freshwater aquaculture. Diad., diadromous. **c**, GHG EI for mariculture finfishes, including these high (>10 kg CO_2e kg^{-1} CW) and low EI (<10 kg CO_2e kg^{-1} CW) species. These high-EI finfishes usually have high FCR (for example, tuna), low edible portion (for example, mullet) and high protein rations in feed (for example, turbot) (Supplementary Table 5). In all panels, data are presented as mean values with 90% CIs (error bars). The sample size varies across species and is larger than 20.

Such a low-O_2 environment can reduce fish fitness[8] and promote the formation of CH_4 and N_2O (ref. 23), which should be avoided when selecting potential mariculture sites. Our freshwater inventory of GHG emissions is associated with a high uncertainty[6,16] because most of these measurements are obtained in the largest aquaculture-producing country China (Source Data Fig. 3), and more observations in other countries are required to better constrain the emissions.

Based on the LCAs, mariculture's GHG footprints are 40–50% lower than freshwater aquaculture, which suggests a large opportunity to mitigate the climate impacts of global blue foods. According to Food and Agriculture Organization (FAO) projections[68], the global demand for fish protein is expected to increase by 14–17% from 2012 to 2050 (Supplementary Fig. 11), with 50–200% increases in Africa and South and Southeast Asia. Given that the wild captures have plateaued since 2000 (ref. 10), if we rely on freshwater systems to feed rising populations, GHG emissions from global aquaculture will probably increase from 410 ± 100 Tg CO_2e yr^{-1} to 600 ± 140 Tg CO_2e yr^{-1} (Supplementary Table 6). If mariculture is utilized to meet these new fish protein needs by the 2050s, it can reduce the emissions from 600 ± 140 to 450 ± 100 Tg CO_2e yr^{-1}. If more aggressive mariculture expansion is adopted, global aquaculture's carbon footprint will be further reduced. For example, in an extreme case in which all fish proteins produced by aquaculture are met by mariculture, the GHG emissions are reduced to 170 ± 40 Tg CO_2e yr^{-1} (assuming the current composition of finfish and bivalve in mariculture farming is maintained), and this requires only 0.083 million km^2 of potential mariculture areas (<1% of the total; Supplementary Table 7). However, replacing freshwater with marine aquaculture needs to consider a lot of socio-economic constraints, including food security, agricultural land use to supply high-protein feed, and infrastructure investment[2]. Nevertheless, mariculture has a 40% lower carbon footprint than the freshwater aquaculture, which has received little attention so far in climate assessment.

Methods

Overview

We developed an approach to estimate GHG emissions intensities arising from mariculture's aquatic environment. Our method is based on the theory of oceanic carbon and nitrogen cycling[23], from which we show that oceanic NPP is the primary fuel of microbial production of CH_4 and N_2O in mariculture regions (depth <200 m) (Supplementary Text 1 and 2 and Supplementary Fig. 7). More specifically, we calculated production efficiencies of CH_4 and N_2O globally at ~10 km resolution using databases of air–sea GHG flux measurements[26,39] and satellite-observed oceanic NPP[28]. Aquafeeds can be considered as human-made NPP added into marine waters, from where we estimated GHG emissions intensity arising from the aquatic environment after considering the transformation of these feeds. We further conducted LCAs to quantify the carbon footprints of freshwater and marine aquaculture.

Global CH_4 and N_2O emissions in offshore mariculture areas

Our global gridded datasets of ocean–atmosphere CH_4 and N_2O fluxes were obtained from Weber et al.[26] and Yang et al.[39], both compiled from research cruise observations from the Marine Methane and NiTrous Oxide (MEMENTO) database and supplemented with recently published measurements from surface ocean waters. These observations are well distributed between marine environments, especially in continental shelf areas. They were interpolated to global grids (at a 25 km resolution) using independent machine learning approaches, with a variety of oceanic physical, chemical and biological properties as predictors. These machine learning methods can reproduce observed N_2O and CH_4 fluxes extremely well (R^2 = 0.7–0.9). According to this dataset, the ocean emits 9 ± 3 Tg yr^{-1} of CH_4 and 6.6 ± 1.6 Tg yr^{-1} of N_2O into the atmosphere. We remapped these datasets to a 10 km resolution for use in this study.

Selection of potentially suitable areas for mariculture

We followed the method of Gentry et al.[8] to select mariculture farming areas that can meet all the following criteria: (1) seafloor depth is less than 200 m based on the bathymetry data from the General Bathymetric Chart of the Oceans (GEBCO) (https://www.gebco.net/); (2) annual dissolved oxygen at 30 m depth or the seafloor (if the maximum depth is less than 30 m)[44] must be above the sublethal limit for fish (4.41 mg l^{-1}); (3) we divided the entire ocean into 30 quantiles based on a global automatic identification system shipping traffic density at the resolution of 10 km (ref. 69) and exclude the areas from the top 1/30 with highest-intensity shipping. Unlike Gentry et al.[8], which excluded the top 1/20 of high-intensity areas, we used a slightly relaxed threshold so that East Asian countries can have more mariculture areas along the coast as reported by previous studies[70]. (4) We determined the suitable growing areas for each of the 160 marine species using their respective upper and lower thermal thresholds based on the maximum

and minimum temperature spanning over 40 years (1982–2019) of sea surface temperature data[71]. Global suitable areas for offshore mariculture are shown in Supplementary Fig. 1.

Database of GHG emission fluxes for three aquaculture types

We conducted literature searches using keywords including 'CH_4 or methane', 'N_2O or nitrous oxide' and 'aquaculture' using Google Scholar and Web of Science until June 2023. We also searched the reference of relevant papers for any additional studies. Finally, we identified 107 observations, including 61 from freshwater systems, 37 from land-based mariculture ponds, and 8 samples from one offshore mariculture bay, and global reconstructed GHG flux (~25 km resolution) from research cruises data[26,39] (Source Data Fig. 3). We also compiled a worldwide database of CH_4 from freshwater aquaculture systems by multiplying these fluxes with aquaculture areas, following the method in Yuan et al.[6]. The global total emissions were 7.2 ± 1.7 Tg yr^{-1} for CH_4 and 29 ± 6 Gg yr^{-1} for N_2O in 2014 (Supplementary Tables 1 and 2). For CH_4, the number of observations used for this inventory is >2 times that in two recent studies[6,16], and the global total emission is comparable to Yuan et al.[6] (6 Tg yr^{-1}) and lower than Rosentreter et al.[16] (14 ± 19 Tg yr^{-1}) (Supplementary Table 2).

N_2O is mainly produced by nitrification in mariculture waters

Here we demonstrate that nitrification, other than denitrification, is the primary pathway of N_2O production in mariculture waters[36,38]. More specifically, we used nitrification N_2O yield[38] and dissolved oxygen mixing ratios[44] in the aphotic zone to estimate N_2O production and emissions. According to Battaglia and Joos[38], the nitrification N_2O yield could be simulated from an empirical model, and the parameters of this model were constrained by a global surface ocean partial pressure N_2O observation dataset (Supplementary Fig. 3), which is written as

$$J(N_2O) = (3.3 \times 10^{-5} + 9.1 \times 10^{-4} \times (0.6e^{83[O_2]} + 0.4e^{25.5[O_2]})) \times J(O_2), \quad (1)$$

where $J(O_2)$ is the O_2 consumption term, which can be estimated as the O_2 demands if all organic matter is oxidized through ammonification and nitrification.

$$J(O_2) = 1.42 \times \text{NPP-C}, \quad (2)$$

where 1.42 is the number of O_2 molecules needed through ammonification and aerobic nitrification of every molecule of organic matter $CH_{\frac{175}{106}}O_{\frac{42}{106}}N_{\frac{16}{106}}P_{\frac{1}{106}}$ (ref. 23), and NPP-C is the mole concentrations of NPP in terms of carbon numbers. According to Dunne et al.[31], the percentages of remineralization rates in the aphotic zone relative to total NPP are 16% in near-shore and 10% in shelf ocean areas.

Supplementary Fig. 5 shows the comparison of the estimated production of N_2O from equations (1) and (2) with observed N_2O fluxes from the ocean to the atmosphere in mariculture areas, which exhibit a very high correlation coefficient ($R = 0.78$). This strongly supports our assumption that microbial nitrification is the dominating pathway for N_2O production, and the NPP is the primary fuel for this process.

Global particle export algorithm

Only organic carbon exported outside of the euphotic zone will participate in the formation of CH_4 and N_2O (ref. 23). In oceanic biogeochemical cycling, the particle export ratio (PE) is used to describe such a process, which refers to the ratio between rapidly sinking particulate organic carbon (POC) from the euphotic zone and net primary production. Increasing PE is usually associated with lower temperature (slower remineralization of particulate matter), lower euphotic zone depth (reduced time in the euphotic zone), and increasing primary productivity[30,31,72]. We used the multi-linear regression fit provided by Dunne et al.[30,31] to estimate the PE, which is given as

$$\text{PE} = -0.0101 \times \text{SST} + 0.0582 \times \ln\left(\frac{\text{NPP}}{Z_{eu}}\right) + 0.419 \quad (3)$$

$$Z_{eu} = 35.9 \times C_{surf}^{-0.287}, \quad (4)$$

where Z_{eu} is the euphotic zone depth (m), C_{surf} is surface chlorophyll concentrations observed by satellites[29] (mg l^{-1}) and SST is sea surface temperature (°C)[71]. This algorithm has been demonstrated to have good performance in modelling observations ($R^2 > 0.6$)[30,31].

The fraction (R_f) of POC fluxes reaching the ocean bottom relative to the total POC at the base of the euphotic zone can be approximated using the 'Martin curve'[73], which is written as

$$R_f = \frac{F_Z}{F_{Z_{eu}}} = \left(\frac{Z}{Z_{eu}}\right)^{-0.858}, \quad (5)$$

where Z is the depth of seafloor, F_Z and $F_{Z_{eu}}$ are POC fluxes at the seafloor and at the base of the euphotic zone. Our calculated fluxes are consistent with previous studies using either observations or modelling approaches (Supplementary Fig. 2b).

CH_4 and N_2O production efficiencies in potential mariculture areas

We used 2010–2019 averaged oceanic net primary production data from Moderate Resolution Imaging Spectroradiometer using the standard Vertically Generalized Production Model algorithm (http://science.oregonstate.edu/ocean.productivity/index.php)[28] at a spatial resolution of 1/12 degrees. The annual phytoplankton carbon fixation rate in this dataset is 48 Pg C yr^{-1} during this period. We assumed the atomic ratio of carbon and nitrogen in marine phytoplankton is 106:16, following the canonical Redfield ratio[74]. We wrote the production efficiencies of CH_4 and N_2O from NPP in mariculture waters as

$$\text{PF}_{CH_4} = \frac{E_{CH_4}}{\text{NPP}} \quad (6)$$

$$\text{PF}_{N_2O} = \frac{E_{N_2O}}{\text{NPP} \times \delta_{N-C}}, \quad (7)$$

where PF_{CH_4} and PF_{N_2O} are the production efficiencies (unitless) of CH_4 and N_2O from NPP, δ_{N-C} is the mass ratio of N to C (0.176) in typical marine phytoplankton[74], NPP is in the unit of carbon mass (g C yr^{-1}), and E_{CH4} (g CH_4–C yr^{-1}) and E_{N_2O} (g N_2O–N yr^{-1}) are emissions of CH_4 and N_2O from the surface ocean to the atmosphere.

GHG emissions intensities from mariculture's aquatic environment

We calculated GHG (CH_4 and N_2O) emissions per kilogram of edible production as follows. First, we converted aquafeeds, excluding the part transformed to fish biomass, to equivalent NPP (or NPP_e). According to aquafeed transformation pathways in the aquaculture system, NPP_e is the sum of solid particulate waste (wasted feeds and faeces, denoted as NPP_{solid}) and newly produced NPP (NPP_{new}) from excreted ammonia[15]. Thus, NPP_e can be written as

$$\text{NPP}_{new} = \frac{1{,}000 \times \text{FCR}}{E_f} \times F_N \times N_{am} \times \frac{1}{\delta_{N-C}} \quad (8)$$

$$\text{NPP}_{solid} = \frac{1{,}000 \times \text{FCR}}{E_f} \times F_C \times C_{solid}, \quad (9)$$

where FCR is the feed conversion ratio, describing the amount of feed required (kg) to produce every kilogram of harvested fish, ranging from 1 to 3 for most fish species (Supplementary Table 5). E_f is the edible fraction of each fish species, N_{am} is the percentage of nitrogen excreted as ammonium through gills (~56%; Supplementary Fig. 6), C_{solid} is the fraction of carbon in particulate waste (~20% in Supplementary Fig. 6, including faeces and wasted food), δ_{N-C} is the mass ratio of N to C (0.176) in NPP[74], and F_N and F_C are the mass fraction of N and C, respectively, in aquafeeds. Second, we calculated GHG emissions by multiplying NPP_e

with the production efficiency on different assumptions of export efficiency of NPP_e to the aphotic zone, which are written as

$$EI_{CH_4,\text{lower bound}} = PF_{CH_4} \times (NPP_{new} + NPP_{solid}) \quad (10)$$

$$EI_{CH_4,\text{upper bound}} = PF_{CH_4} \times \left(\frac{NPP_{new}}{PE} + \frac{NPP_{solid}}{R_f \times PE}\right) \quad (11)$$

$$EI_{N_2O,\text{lower bound}} = PF_{N_2O} \times (NPP_{new} \times \delta_{N-C}) \quad (12)$$

$$EI_{N_2O,\text{upper bound}} = PF_{N_2O} \times \frac{NPP_{new} \times \delta_{N-C}}{PE}, \quad (13)$$

where EI_{CH4} (g CH_4 kg^{-1} CW) and EI_{N2O} (g N_2O kg^{-1} CW) are emissions intensities of CH_4 and N_2O from every kilogram of edible fish production, PF_{CH_4} and PF_{N_2O} are the production efficiencies (unitless) from equations (6) and (7), and R_f is from equation (5). For the lower bound, we assumed that all NPP_e resembles the behaviours of NPP, which means ~26% of NPP_e is exported into aphotic zones and participates in the biochemical production of CH_4 and N_2O (Supplementary Fig. 8a). For the upper bound, we assumed all NPP_{solid} can quickly sink to the seafloor, and all NPP_{new} can enter the aphotic zone (Supplementary Fig. 8b).

Carbon footprint analysis of global aquaculture

The goal of the LCA presented here is to evaluate the carbon footprints between freshwater aquaculture and mariculture. The brackish aquaculture has varying salinities that may cause the aquatic methane emissions intensity to be different by a factor of 10 (Fig. 3a); thus, it is not considered in this analysis because there are no reported salinity data for coastal ponds at the global scale.

This LCA encompasses 23 farmed species groups, which account for >90% of global aquaculture production in 2021. The system boundary is 'cradle to farm-gate', which can be divided into three main parts: feed production, energy use and aquatic environment emissions. For non-aquatic GHG emissions, the technical details are mainly based on two recent studies, MacLeod et al.[11] and Gephart et al.[63], supplemented with updated data to improve underrepresented species groups, such as tuna, amberjack and barramundi. GHG from feed includes the production and use of fertilizers, land use change, crop energy use, crop N_2O and rice CH_4, processing and transportation, animal-based ingredients (for example, fishmeal and fish oil) and other materials (for example, vitamin and mineral). The emission factors for feed are based on MacLeod et al.[11], using the values derived by the Global Livestock Environmental Assessment Model[75] with detailed regional and species variations. On-farm energy use, primarily for pumping water, lighting, powering vehicles and processing, is from Gephart et al.[63]. FCRs are based on Gephart et al.[63], with new literature searches for better speciation. Production data are extracted from the FAO database FishStatJ for 2021 (ref. 76). Overall, our inter-species EIs are consistent with results in Gephart et al.[63], and the correlation coefficient is 0.92 (Supplementary Fig. 12a). Of all covariates, the three leading factors—FCR, total protein content in feed and the fraction of high-quality protein in feed—can explain 94% of the inter-species variations using a linear regression model (Supplementary Fig. 12b).

Distinct from previous literature, this LCA includes GHG emissions from the aquatic environment during cultivation. For freshwater aquaculture, we complied a new emission inventory of CH_4 and N_2O from 67 and 49 observations (Supplementary Tables 1 and 2), and the EI is obtained via dividing these emissions by the edible portion of global aquaculture products (Supplementary Table 3). For mariculture, we used the EI calculated by this study (Figs. 3 and 4).

Uncertainty assessment

To quantify the overall uncertainty of these trajectories, we conducted an ensemble of experiments with different assumptions on error statistics for each subprocess (Supplementary Table 8). (1) For CH_4 and N_2O emissions emitted by the ocean at the global scale, we assumed a relative uncertainty (1σ) of 17% and 12%, respectively, as provided by Weber et al.[26] and Yang et al.[39]. (2) For CH_4 and N_2O emissions intensity arising from the aquatic environment of freshwater systems, the relative uncertainties (1σ) were 14% and 11% derived from 1,000 Monte Carlo experiments. (3) The relative uncertainty of N_{am} (the percentage of nitrogen excreted as ammonium through gills) was assumed to be 6% (1σ), using the same uncertainty value of nitrogen utilization efficiency in aquaculture[15]. (4) For FCR, the inter-species standard deviation is 0.3, which was also used by each individual species. (5) The fraction of NPP exported out of the euphotic zone was calculated using the particle export ratio[30,31] or assumed to be 100% (see Supplementary Fig. 8 for details). Finally, we used the Monte Carlo method to sample from all possible experiments and report errors as 90% CIs.

Statistics and reproducibility

All data collected from previous literature are used in the analyses. No statistical method was used to pre-determine the sample size. The experiments were not randomized. The investigators were not blinded to allocation during experiments and outcome assessment. R version 4.2.2 was used for data analysis, and the scripts are available in the data repository as indicated in 'Code availability'.

Reporting summary

Further information on research design is available in the Nature Portfolio Reporting Summary linked to this article.

Data availability

All data used in the analyses are clearly cited in Methods. Source data are provided with this paper. The data used to reproduce the main findings of this work are available at https://doi.org/10.18170/DVN/ZWJWCD. Other supporting data are available in Supplementary Information.

Code availability

The analysis is mainly conducted using the open-source software R version 4.2.2. The code used to reproduce the main finding and figures of this work can be obtained at https://doi.org/10.18170/DVN/ZWJWCD.

References

1. Free, C. M. et al. Expanding ocean food production under climate change. *Nature* **605**, 490–496 (2022).
2. Zhang, W. et al. Aquaculture will continue to depend more on land than sea. *Nature* **603**, E2–E4 (2022).
3. *FAO Yearbook. Fishery and Aquaculture Statistics 2019. Rome, Statistics and Information Service of the Fisheries and Aquaculture Department* (FAO, 2021).
4. Cole, D. W. et al. Aquaculture: environmental, toxicological, and health issues. *Int. J. Hyg. Environ. Health* **212**, 369–377 (2009).
5. Cao, L. et al. China's aquaculture and the world's wild fisheries. *Science* **347**, 133–135 (2015).
6. Yuan, J. et al. Rapid growth in greenhouse gas emissions from the adoption of industrial-scale aquaculture. *Nat. Clim. Change* **9**, 318–322 (2019).
7. Merino, G. et al. Can marine fisheries and aquaculture meet fish demand from a growing human population in a changing climate? *Glob. Environ. Change* **22**, 795–806 (2012).
8. Gentry, R. R. et al. Mapping the global potential for marine aquaculture. *Nat. Ecol. Evol.* **1**, 1317–1324 (2017).
9. Froehlich, H. E., Gentry, R. R. & Halpern, B. S. Global change in marine aquaculture production potential under climate change. *Nat. Ecol. Evol.* **2**, 1745–1750 (2018).
10. Costello, C. et al. The future of food from the sea. *Nature* **588**, 95–100 (2020).

11. MacLeod, M. J., Hasan, M. R., Robb, D. H. F. & Mamun-Ur-Rashid, M. Quantifying greenhouse gas emissions from global aquaculture. *Sci. Rep.* **10**, 11679 (2020).
12. Jones, A. R. et al. Climate-friendly seafood: the potential for emissions reduction and carbon capture in marine aquaculture. *BioScience* **72**, 123–143 (2022).
13. Naylor, R. L. et al. Effect of aquaculture on world fish supplies. *Nature* **405**, 1017–1024 (2000).
14. Hargreaves, J. A. Nitrogen biogeochemistry of aquaculture ponds. *Aquaculture* **166**, 181–212 (1998).
15. Hu, Z., Lee, J. W., Chandran, K., Kim, S. & Khanal, S. K. Nitrous oxide (N_2O) emission from aquaculture: a review. *Environ. Sci. Technol.* **46**, 6470–6480 (2012).
16. Rosentreter, J. A. et al. Half of global methane emissions come from highly variable aquatic ecosystem sources. *Nat. Geosci.* **14**, 225–230 (2021).
17. Williams, J. & Crutzen, P. J. Nitrous oxide from aquaculture. *Nat. Geosci.* **3**, 143–143 (2010).
18. Yang, P. et al. Insights into the farming-season carbon budget of coastal earthen aquaculture ponds in southeastern China. *Agric. Ecosyst. Environ.* **335**, 107995 (2022).
19. Naylor, R. L. et al. A 20-year retrospective review of global aquaculture. *Nature* **591**, 551–563 (2021).
20. Rubino, M. *Offshore Aquaculture in the United States: Economic Considerations, Implications and Opportunities* (US Department of Commerce National Oceanic and Atmospheric Administration, 2008).
21. Parodi, A. et al. The potential of future foods for sustainable and healthy diets. *Nat. Sustain.* **1**, 782–789 (2018).
22. Ray, N. E., Maguire, T. J., Al-Haj, A. N., Henning, M. C. & Fulweiler, R. W. Low greenhouse gas emissions from oyster aquaculture. *Environ. Sci. Technol.* **53**, 9118–9127 (2019).
23. Capone, D. G., Bronk, D. A., Mulholland, M. R. & Carpenter, E. J. *Nitrogen in the Marine Environment* (Elsevier, 2008).
24. Reeburgh, W. S. Oceanic methane biogeochemistry. *Chem. Rev.* **107**, 486–513 (2007).
25. Bastviken, D., Cole, J. J., Pace, M. L. & Van de Bogert, M. C. Fates of methane from different lake habitats: connecting whole-lake budgets and CH_4 emissions. *J. Geophys. Res. Biogeosci.* **113**, G02024 (2008).
26. Weber, T., Wiseman, N. A. & Kock, A. Global ocean methane emissions dominated by shallow coastal waters. *Nat. Commun.* **10**, 4584 (2019).
27. Li, M. et al. The significant contribution of lake depth in regulating global lake diffusive methane emissions. *Water Res.* **172**, 115465 (2020).
28. Behrenfeld, M. J. & Falkowski, P. G. Photosynthetic rates derived from satellite-based chlorophyll concentration. *Limnol. Oceanogr.* **42**, 1–20 (1997).
29. Ancillary data sources. *NASA Ocean Biology Processing Group* https://oceancolor.gsfc.nasa.gov/l3/order/ (2023).
30. Dunne, J. P., Armstrong, R. A., Gnanadesikan, A. & Sarmiento, J. L. Empirical and mechanistic models for the particle export ratio. *Glob. Biogeochem. Cycles* **19**, GB4026 (2005).
31. Dunne, J. P., Sarmiento, J. L. & Gnanadesikan, A. A synthesis of global particle export from the surface ocean and cycling through the ocean interior and on the seafloor. *Glob. Biogeochem. Cycles* **21**, GB4006 (2007).
32. Zhao, J. et al. Large methane emission from freshwater aquaculture ponds revealed by long-term eddy covariance observation. *Agric. For. Meteorol.* **308–309**, 108600 (2021).
33. Lovley, D. R. & Klug, M. J. Sulfate reducers can outcompete methanogens at freshwater sulfate concentrations. *Appl. Environ. Microbiol.* **45**, 187–192 (1983).
34. Winfrey, M. R. & Zeikus, J. G. Effect of sulfate on carbon and electron flow during microbial methanogenesis in freshwater sediments. *Appl. Environ. Microbiol.* **33**, 275–281 (1977).
35. Jin, X. & Gruber, N. Offsetting the radiative benefit of ocean iron fertilization by enhancing N_2O emissions. *Geophys. Res. Lett.* **30**, 2249 (2003).
36. Nevison, C., Butler, J. H. & Elkins, J. W. Global distribution of N_2O and the ΔN_2O-AOU yield in the subsurface ocean. *Glob. Biogeochem. Cycles* **17**, 1119 (2003).
37. Suntharalingam, P. & Sarmiento, J. L. Factors governing the oceanic nitrous oxide distribution: simulations with an ocean general circulation model. *Glob. Biogeochem. Cycles* **14**, 429–454 (2000).
38. Battaglia, G. & Joos, F. Marine N_2O emissions from nitrification and denitrification constrained by modern observations and projected in multimillennial global warming simulations. *Glob. Biogeochem. Cycles* **32**, 92–121 (2018).
39. Yang, S. et al. Global reconstruction reduces the uncertainty of oceanic nitrous oxide emissions and reveals a vigorous seasonal cycle. *Proc. Natl. Acad. Sci. USA* **117**, 11954–11960 (2020).
40. Resplandy, L. et al. A synthesis of global coastal ocean greenhouse gas fluxes. *Glob. Biogeochem. Cycles* **38**, e2023GB007803 (2024).
41. Arévalo-Martínez, D. L. et al. N_2O emissions from the northern Benguela upwelling system. *Geophys. Res. Lett.* **46**, 3317–3326 (2019).
42. Arévalo-Martínez, D. L., Kock, A., Löscher, C. R., Schmitz, R. A. & Bange, H. W. Massive nitrous oxide emissions from the tropical South Pacific Ocean. *Nat. Geosci.* **8**, 530–533 (2015).
43. Yang, S., Gruber, N., Long, M. C. & Vogt, M. ENSO-driven variability of denitrification and suboxia in the eastern tropical Pacific ocean. *Glob. Biogeochem. Cycles* **31**, 1470–1487 (2017).
44. Garcia, H. E. et al. World Ocean Atlas 2018, Volume 3: Dissolved Oxygen, Apparent Oxygen Utilization, and Dissolved Oxygen Saturation (National Oceanic and Atmospheric Administration, 2019).
45. Olsen, L. M., Holmer, M. & Olsen, Y. Perspectives of nutrient emission from fish aquaculture in coastal waters. Literature review with evaluated state of knowledge. *FHF Project* **542014**, 87 (2008).
46. Zhu, Y. et al. Disproportionate increase in freshwater methane emissions induced by experimental warming. *Nat. Clim. Change* **10**, 685–690 (2020).
47. Vanzella, A., Guerrero, M. & Jones, R. Effect of CO and light on ammonium and nitrite oxidation by chemolithotrophic bacteria. *Mar. Ecol. Prog. Ser.* **57**, 69–76 (1989).
48. Horrigan, S. G. & Springer, A. L. Oceanic and estuarine ammonium oxidation: effects of light. *Limnol. Oceanogr.* **35**, 479–482 (1990).
49. Hou, J., Zhang, G., Sun, M., Ye, W. & Song, D. Methane distribution, sources, and sinks in an aquaculture bay (Sanggou Bay, China). *Aquac. Environ. Interact.* **8**, 481–495 (2016).
50. Saunois, M. et al. The Global Methane Budget 2000–2017. *Earth Syst. Sci. Data* **12**, 1561–1623 (2020).
51. Yang, P. et al. Large variations in indirect N_2O emission factors (EF5) from coastal aquaculture systems in China from plot to regional scales. *Water Res.* **200**, 117208 (2021).
52. Yang, P. et al. Environmental drivers of nitrous oxide emission factor for a coastal reservoir and its catchment areas in southeastern China. *Environ. Pollut.* **294**, 118568 (2022).
53. Fagodiya, R. K. et al. Greenhouse gas emissions from salt-affected soils: mechanistic understanding of interplay factors and reclamation approaches. *Sustainability* **14**, 11876 (2022).
54. Wang, X. et al. Seasonal variations of nitrous oxide fluxes and soil denitrification rates in subtropical freshwater and brackish tidal marshes of the Min River estuary. *Sci. Total Environ.* **616–617**, 1404–1413 (2018).
55. Welti, N., Hayes, M. & Lockington, D. Seasonal nitrous oxide and methane emissions across a subtropical estuarine salinity gradient. *Biogeochemistry* **132**, 55–69 (2017).

56. von Ahnen, M., Aalto, S. L., Suurnäkki, S., Tiirola, M. & Pedersen, P. B. Salinity affects nitrate removal and microbial composition of denitrifying woodchip bioreactors treating recirculating aquaculture system effluents. *Aquaculture* **504**, 182–189 (2019).
57. Li, Y. et al. Enhanced N_2O production induced by soil salinity at a specific range. *Int. J. Environ. Res. Public Health* **17**, 5169 (2020).
58. Gauci, V. et al. Sulfur pollution suppression of the wetland methane source in the 20th and 21st centuries. *Proc. Natl. Acad. Sci. USA* **101**, 12583–12587 (2004).
59. Pester, M. Sulfate-reducing microorganisms in wetlands—fameless actors in carbon cycling and climate change. *Front. Microbiol.* **3**, 72 (2012).
60. Pakulski, J. D. et al. Microbial metabolism and nutrient cycling in the Mississippi and Atchafalaya River plumes. *Estuar. Coast. Shelf Sci.* **50**, 173–184 (2000).
61. Magalhães, C. M., Joye, S. B., Moreira, R. M., Wiebe, W. J. & Bordalo, A. A. Effect of salinity and inorganic nitrogen concentrations on nitrification and denitrification rates in intertidal sediments and rocky biofilms of the Douro River estuary, Portugal. *Water Res.* **39**, 1783–1794 (2005).
62. Zhou, M., Butterbach-Bahl, K., Vereecken, H. & Brüggemann, N. A meta-analysis of soil salinization effects on nitrogen pools, cycles and fluxes in coastal ecosystems. *Glob. Change Biol.* **23**, 1338–1352 (2017).
63. Gephart, J. A. et al. Environmental performance of blue foods. *Nature* **597**, 360–365 (2021).
64. Yue, K. & Shen, Y. An overview of disruptive technologies for aquaculture. *Aquac. Fish.* **7**, 111–120 (2022).
65. Costa-Pierce, B. A. in *Ecology as the Paradigm for the Future of Aquaculture* (ed. Costa-Pierce, B. A.) 337–372 (Blackwell Science, 2002).
66. Okin, G. S. et al. Impacts of atmospheric nutrient deposition on marine productivity: roles of nitrogen, phosphorus, and iron. *Glob. Biogeochem. Cycles* **25**, GB2022 (2011).
67. Dai, Y. et al. Coastal phytoplankton blooms expand and intensify in the 21st century. *Nature* **615**, 280–284 (2023).
68. *The Future of Food and Agriculture—Alternative Pathways to 2050* (FAO, 2018).
69. Wu, L., Xu, Y., Wang, Q., Wang, F. & Xu, Z. Mapping global shipping density from AIS data. *J. Navig.* **70**, 67–81 (2017).
70. Akber, Md. A., Aziz, A. A. & Lovelock, C. Major drivers of coastal aquaculture expansion in Southeast Asia. *Ocean Coast. Manag.* **198**, 105364 (2020).
71. Reynolds, R. W. et al. Daily high-resolution-blended analyses for sea surface temperature. *J. Climate* **20**, 5473–5496 (2007).
72. Friedland, K. D. et al. Pathways between primary production and fisheries yields of large marine ecosystems. *PLoS ONE* **7**, e28945 (2012).
73. Martin, J. H., Knauer, G. A., Karl, D. M. & Broenkow, W. W. VERTEX: carbon cycling in the northeast Pacific. *Deep Sea Res. Part Oceanogr. Res. Pap.* **34**, 267–285 (1987).
74. Redfield, A. C. The biological control of chemical factors in the environment. *Am. Sci.* **46**, 205–221 (1958).
75. *Global Livestock Environmental Assessment Model (GLEAM)* (FAO, 2017).
76. *FishStatJ—Software for Fishery and Aquaculture Statistical Time Series* (FAO Fisheries and Aquaculture Department, 2022).

Acknowledgements

This work was supported by National Key Research and Development Program of China (2023YFC3707404, L.S.) and the National Natural Science Foundation of China (42275194, L.S.). We thank H. Liu from Tsinghua University, Y. Yu from Peking University, Y. Zhang from Texas A&M University and Y. Li from Baylor University for the fruitful discussion of this work.

Author contributions

L.S. conceived the study and wrote the paper. L.S., Lidong W. and M.Z. designed the experiments, and L.S. carried them out. W.W. conducted the life cycle analysis. Y.Y., J.L., G.S. and M.L. contributed to the interpretation of results. M.L., G.S., J.Y. and Lin W. contributed to the acquisition and analysis of data. L.S. prepared the paper with contributions from all co-authors. Y.Y. and M.Z. revised the paper.

Competing interests

The authors declare no competing interests.

Additional information

Supplementary information The online version contains supplementary material available at https://doi.org/10.1038/s43016-024-01004-y.

Correspondence and requests for materials should be addressed to Lu Shen or Minghao Zhuang.

Peer review information *Nature Food* thanks Damian Arévalo-Martínez, Patrik Henriksson, Michael Krom and Richard Newton for their contribution to the peer review of this work.

Reprints and permissions information is available at www.nature.com/reprints.

Publisher's note Springer Nature remains neutral with regard to jurisdictional claims in published maps and institutional affiliations.

[1]Department of Atmospheric and Oceanic Sciences, School of Physics, Peking University, Beijing, China. [2]Institute of Carbon Neutrality, Peking University, Beijing, China. [3]Chinese Academy of Fishery Sciences, Beijing, China. [4]State Key Laboratory of Mariculture Biobreeding and Sustainable Goods, Chinese Academy of Fishery Sciences, Qingdao, China. [5]Key Laboratory of the Three Gorges Reservoir Region's Eco-Environment, Ministry of Education, Chongqing University, Chongqing, China. [6]Department of Rural Economy, Environment and Society, Scotland's Rural College, Edinburgh, UK. [7]Frontiers Science Center for Deep Ocean Multispheres and Earth System and Key Laboratory of Marine Chemistry Theory and Technology (Ministry of Education), Ocean University of China, Qingdao, China. [8]State Key Laboratory of Soil and Sustainable Agriculture, Institute of Soil Science, Chinese Academy of Sciences, Nanjing, China. [9]School of Geographical Sciences, Fujian Normal University, Fuzhou, China. [10]Institute of Computing Technology, Chinese Academy of Sciences, Beijing, China. [11]Institute of Energy, Environment and Economy, Tsinghua University, Beijing, China. [12]State Key Laboratory of Nutrient Use and Management, College of Resources and Environmental Sciences, Key Laboratory of Plant-Soil Interactions, Ministry of Education, China Agricultural University, Beijing, China. [13]These authors contributed equally: Lu Shen, Lidong Wu, Wei Wei.
✉e-mail: lshen@pku.edu.cn; zhuangminghao@cau.edu.cn

nature portfolio

Corresponding author(s): Lu Shen, Minghao Zhuang

Last updated by author(s): Apr 23, 2024

Reporting Summary

Nature Portfolio wishes to improve the reproducibility of the work that we publish. This form provides structure for consistency and transparency in reporting. For further information on Nature Portfolio policies, see our Editorial Policies and the Editorial Policy Checklist.

Statistics

For all statistical analyses, confirm that the following items are present in the figure legend, table legend, main text, or Methods section.

n/a	Confirmed
☐	☒ The exact sample size (*n*) for each experimental group/condition, given as a discrete number and unit of measurement
☐	☒ A statement on whether measurements were taken from distinct samples or whether the same sample was measured repeatedly
☐	☒ The statistical test(s) used AND whether they are one- or two-sided *Only common tests should be described solely by name; describe more complex techniques in the Methods section.*
☐	☒ A description of all covariates tested
☐	☒ A description of any assumptions or corrections, such as tests of normality and adjustment for multiple comparisons
☐	☒ A full description of the statistical parameters including central tendency (e.g. means) or other basic estimates (e.g. regression coefficient) AND variation (e.g. standard deviation) or associated estimates of uncertainty (e.g. confidence intervals)
☐	☒ For null hypothesis testing, the test statistic (e.g. *F*, *t*, *r*) with confidence intervals, effect sizes, degrees of freedom and *P* value noted *Give P values as exact values whenever suitable.*
☐	☒ For Bayesian analysis, information on the choice of priors and Markov chain Monte Carlo settings
☐	☒ For hierarchical and complex designs, identification of the appropriate level for tests and full reporting of outcomes
☒	☐ Estimates of effect sizes (e.g. Cohen's *d*, Pearson's *r*), indicating how they were calculated

Our web collection on statistics for biologists contains articles on many of the points above.

Software and code

Policy information about availability of computer code

Data collection	We conducted literature searches using keywords including 'CH4 or methane', 'N2O or nitrous oxide', and 'aquaculture' using Google Scholar and Web of Science in June 2023. No software is used for data collection here. Fish production were obtained from FishStatJ – Software for Fishery and Aquaculture Statistical Time Series (https://www.fao.org/fishery/en/statistics/software/fishstatj/en). Future projection of fish protein needs are from FAO (https://www.fao.org/global-perspectives-studies/food-agriculture-projections-to-2050/en/). All data are publicly accessible.
Data analysis	We use R v4.2.2 (open-source) as the major data analysis software in this study.

For manuscripts utilizing custom algorithms or software that are central to the research but not yet described in published literature, software must be made available to editors and reviewers. We strongly encourage code deposition in a community repository (e.g. GitHub). See the Nature Portfolio guidelines for submitting code & software for further information.

Data

Policy information about availability of data

All manuscripts must include a data availability statement. This statement should provide the following information, where applicable:

- Accession codes, unique identifiers, or web links for publicly available datasets
- A description of any restrictions on data availability
- For clinical datasets or third party data, please ensure that the statement adheres to our policy

All data used in the analyses are clearly cited in the Methods. Fish production is from FishStatJ – Software for Fishery and Aquaculture Statistical Time Series (https://www.fao.org/fishery/en/statistics/software/fishstatj/en). The databases of the two meta-analyses are available as Extended Datasets linked to this article. The data used to reproduce the main findings of this work are available at https://doi.org/10.18170/DVN/ZWJWCD. Other supporting data are available in the Supplementary Information.

Research involving human participants, their data, or biological material

Policy information about studies with human participants or human data. See also policy information about sex, gender (identity/presentation), and sexual orientation and race, ethnicity and racism.

Reporting on sex and gender	n/a
Reporting on race, ethnicity, or other socially relevant groupings	n/a
Population characteristics	n/a
Recruitment	n/a
Ethics oversight	n/a

Note that full information on the approval of the study protocol must also be provided in the manuscript.

Field-specific reporting

Please select the one below that is the best fit for your research. If you are not sure, read the appropriate sections before making your selection.

☐ Life sciences ☐ Behavioural & social sciences ☒ Ecological, evolutionary & environmental sciences

For a reference copy of the document with all sections, see nature.com/documents/nr-reporting-summary-flat.pdf

Ecological, evolutionary & environmental sciences study design

All studies must disclose on these points even when the disclosure is negative.

Study description	Based on the theory of ocean geochemical cycling, we develop the first approach to map global GHG emission intensity from mariculture's aquatic environment at ~10km resolution, using data from research cruises and satellites. We also conduct a life-cycle assessment to estimate mariculture's carbon footprints.
Research sample	We estimate that mariculture's aquatic emission intensities are estimated to be 1–6 gCH4kg-1CW (carcass weight) and 0.05–0.2 gN2Okg-1CW.
Sampling strategy	To quantify the overall uncertainty of these trajectories, we conduct an ensemble of experiments with different assumptions on error statistics for each subprocess. Finally, we use the Monte Carlo method to sample from all possible experiments and report errors as one standard deviation.
Data collection	Our global gridded datasets of ocean-atmosphere CH4 and N2O fluxes are obtained from Weber et al.25 and Yang et al.37, both compiled from research cruise observations from the Marine Methane and NiTrous Oxide (MEMENTO) database and supplemented with recently published measurements from surface ocean waters. We compiled the GHG emission intensity database for three different aquaculture types from recently published data and this work. This life cycle assessment (LCA) encompasses 23 farmed species groups, which account for >90% of global aquaculture production in 2021. For non-aquatic GHG emissions, the technical details are mainly based on two recent studies MacLeod et al.11 and Gephart et al.59, supplemented with updated data to improve underrepresented species groups.
Timing and spatial scale	Until June 2023; globally
Data exclusions	We have kept all available data that is peer-reviewed.

Reproducibility	All data, code, and materials used in the analyses are available at https://doi.org/10.18170/DVN/ZWJWCD.
Randomization	We use the Monte Carlo method to sample from all possible experiments. Given the large number of samples, randomization doesn't seem to affect the conclusion.
Blinding	n/a

Did the study involve field work? ☐ Yes ☒ No

Reporting for specific materials, systems and methods

We require information from authors about some types of materials, experimental systems and methods used in many studies. Here, indicate whether each material, system or method listed is relevant to your study. If you are not sure if a list item applies to your research, read the appropriate section before selecting a response.

Materials & experimental systems

n/a	Involved in the study
☒	☐ Antibodies
☒	☐ Eukaryotic cell lines
☒	☐ Palaeontology and archaeology
☒	☐ Animals and other organisms
☒	☐ Clinical data
☒	☐ Dual use research of concern
☒	☐ Plants

Methods

n/a	Involved in the study
☒	☐ ChIP-seq
☒	☐ Flow cytometry
☒	☐ MRI-based neuroimaging

Plants

Seed stocks	n/a
Novel plant genotypes	n/a
Authentication	n/a

Terms and Conditions

Springer Nature journal content, brought to you courtesy of Springer Nature Customer Service Center GmbH (“Springer Nature”).
Springer Nature supports a reasonable amount of sharing of research papers by authors, subscribers and authorised users (“Users”), for small-scale personal, non-commercial use provided that all copyright, trade and service marks and other proprietary notices are maintained. By accessing, sharing, receiving or otherwise using the Springer Nature journal content you agree to these terms of use (“Terms”). For these purposes, Springer Nature considers academic use (by researchers and students) to be non-commercial.
These Terms are supplementary and will apply in addition to any applicable website terms and conditions, a relevant site licence or a personal subscription. These Terms will prevail over any conflict or ambiguity with regards to the relevant terms, a site licence or a personal subscription (to the extent of the conflict or ambiguity only). For Creative Commons-licensed articles, the terms of the Creative Commons license used will apply.
We collect and use personal data to provide access to the Springer Nature journal content. We may also use these personal data internally within ResearchGate and Springer Nature and as agreed share it, in an anonymised way, for purposes of tracking, analysis and reporting. We will not otherwise disclose your personal data outside the ResearchGate or the Springer Nature group of companies unless we have your permission as detailed in the Privacy Policy.
While Users may use the Springer Nature journal content for small scale, personal non-commercial use, it is important to note that Users may not:

1. use such content for the purpose of providing other users with access on a regular or large scale basis or as a means to circumvent access control;
2. use such content where to do so would be considered a criminal or statutory offence in any jurisdiction, or gives rise to civil liability, or is otherwise unlawful;
3. falsely or misleadingly imply or suggest endorsement, approval , sponsorship, or association unless explicitly agreed to by Springer Nature in writing;
4. use bots or other automated methods to access the content or redirect messages
5. override any security feature or exclusionary protocol; or
6. share the content in order to create substitute for Springer Nature products or services or a systematic database of Springer Nature journal content.

In line with the restriction against commercial use, Springer Nature does not permit the creation of a product or service that creates revenue, royalties, rent or income from our content or its inclusion as part of a paid for service or for other commercial gain. Springer Nature journal content cannot be used for inter-library loans and librarians may not upload Springer Nature journal content on a large scale into their, or any other, institutional repository.
These terms of use are reviewed regularly and may be amended at any time. Springer Nature is not obligated to publish any information or content on this website and may remove it or features or functionality at our sole discretion, at any time with or without notice. Springer Nature may revoke this licence to you at any time and remove access to any copies of the Springer Nature journal content which have been saved.
To the fullest extent permitted by law, Springer Nature makes no warranties, representations or guarantees to Users, either express or implied with respect to the Springer nature journal content and all parties disclaim and waive any implied warranties or warranties imposed by law, including merchantability or fitness for any particular purpose.
Please note that these rights do not automatically extend to content, data or other material published by Springer Nature that may be licensed from third parties.
If you would like to use or distribute our Springer Nature journal content to a wider audience or on a regular basis or in any other manner not expressly permitted by these Terms, please contact Springer Nature at

onlineservice@springernature.com